



## Energy and mass assessment of the laser Directed Energy Deposition process (DED-LB) for reduced environmental impact

J.I. Arrizubieta, O. Murua, A. Urresti & O. Ukar

**To cite this article:** J.I. Arrizubieta, O. Murua, A. Urresti & O. Ukar (2024) Energy and mass assessment of the laser Directed Energy Deposition process (DED-LB) for reduced environmental impact, International Journal of Sustainable Engineering, 17:1, 1-11, DOI: [10.1080/19397038.2024.2316125](https://doi.org/10.1080/19397038.2024.2316125)

**To link to this article:** <https://doi.org/10.1080/19397038.2024.2316125>



© 2024 The Author(s). Published by Informa UK Limited, trading as Taylor & Francis Group.



Published online: 18 Feb 2024.



Submit your article to this journal [↗](#)



Article views: 556



View related articles [↗](#)



View Crossmark data [↗](#)

# Energy and mass assessment of the laser Directed Energy Deposition process (DED-LB) for reduced environmental impact

J.I. Arrizubieta <sup>a</sup>, O. Murua <sup>a</sup>, A. Urresti <sup>a</sup> and O. Ukar <sup>b</sup>

<sup>a</sup>Department of Mechanical Engineering, University of the Basque Country, Bilbao, Spain; <sup>b</sup>Department of Mechanics, Design and Industrial Management, University of Deusto, Bilbao, Spain

## ABSTRACT

Additive Manufacturing (AM) processes have the capability to promote a more rational use of resources, reduce generated waste, as well as repair damaged components to extend their lifespan. With the aim of contributing to a more efficient and environmentally friendlier manufacturing process, this research work investigates the energy consumption of the Laser Directed Energy Deposition process (DED-LB) through the introduction of new parameters in its characterisation, which are energy and mass efficiency. First, the energy efficiency of the laser generator itself has been characterised. Based on the results obtained, it was possible to conclude that pulsed laser operation strategies allow a reduction in consumption of up to 9% compared to a continuous laser operation mode. Second, a design of experiments was carried out to relate the energy and mass efficiency of the deposition process to the input parameters: laser power, feed rate, and mass rate. The parameter that most influences the energy efficiency of the process is the mass rate, where high rates are advisable to maximise its value. On the other hand, it is concluded that an increase in the mass rate or a reduction in the feed rate results in an increase in the mass efficiency

## ARTICLE HISTORY

Received 27 November 2023  
Accepted 31 January 2024

## KEYWORDS

Additive manufacturing;  
directed energy deposition;  
mass efficiency; energy  
efficiency

## 1. Introduction

The manufacturing industry represents one of the main pillars of growth and development for countries, being a position expected to be maintained as the price of the resources and raw materials rise. Likewise, the impact of industry on the development of the economy worldwide and the welfare of society is undeniable (Maddison 2007). Nonetheless, these productive activities also imply a significant resource demand on the environment, quantified by indicators such as air quality, water pollution and resource depletion, and represent a threat to human well-being. Therefore, the productive process implementation and the adoption of manufacturing strategies that minimise this environmental impact become vitally important nowadays.

In this respect, the additive manufacturing (AM) processes have meant a change in the paradigm of productive processes, presenting numerous benefits and advantages when compared to more traditional processes such as machining, forging, or casting. For example, a recent research study explored the possible synergies between the capabilities of AM and the improvement of performance as defined by Green Supply Chain Management criteria (Ferreira et al. 2023). The results supported the potential for cost savings and waste reduction by integrating AM processes in repair applications. From a resource efficiency perspective, AM allows a more rational use of materials, a reduction of the generated waste, as well as the repair of damaged components in order to increase their lifetime (Arrizubieta et al. 2020). In terms of mechanical properties, many studies show that AM processes can result in advanced-performance materials for diverse application areas

such as memory-shaped alloys (Felice et al. 2023). However, AM is not exempt from disadvantages and limitations which have hampered its implementation in sectors such as the automotive and aeronautic industries. One of the main limitations is its low productivity, what makes the AM process become the bottleneck in production lines. For that reason, during the last years the trend has been to increase the power of the equipment and raise the number of nozzles or lasers. Traditionally, the tuning of the AM processes has been performed with the aim of maximising productivity, understood as the amount of material that is deposited per unit of time (Schwerz et al. 2022), neglecting the environmental impact of these parameters and the efficiency of the process itself.

The standard (ISO/ASTM 52900: 2021) defines additive manufacturing as a set of processes based on the addition principle that permit obtaining three-dimensional components by successive material addition (ISO/ASTM 2021). Therefore, the different additive manufacturing processes are classified according to the material they work with and the applied technology for the material addition. The principal metallic additive manufacturing technologies are the processes of laser Powder Bed Fusion (PBF-LB), laser Directed Energy Deposition (DED-LB) and Binder Jetting (BJT).

Focusing this study on the DED-LB, this process offers advantages such as the geometrical design flexibility and the possibility of manufacturing components with integrated functionality through multimaterial strategies. In this regard, it is possible to vary the composition of the component gradually, creating what is known as Functionally Graded Materials (FGM). Therefore, this process can be highly profitable in the manufacture of small

production batches and customised components, as well as allowing for efficient use of material and energy (Tan et al. 2021). Regarding the last characteristic, numerous successful cases have been reported in which AM has enabled a reduction of waste material (Najmon, Raesi, and Tovar 2019; Nickels 2015). However, when referring to energy savings, most authors refer to saves introduced by the optimised design over the lifetime of the component, leaving aside the energy consumption of the manufacturing process itself.

As described by Ehmsen et al., there are three categories of research works related to energy consumption in AM processes (Ehmsen, Glatt, and Aurich 2023). First, some works are focused on evaluating the energy consumption of DED-LB experimentally (Huang et al. 2016; Jackson et al. 2016; Wippermann et al. 2020). Although they consider different scenarios, they do not analyse in depth which parameters affect energy demand. Second, other works analyse the energy consumption in different types of AM processes and study the energy demand of each individual process element (Khalid and Peng 2021; Peng et al. 2021; Yang et al. 2017). Third, the influence of DED-LB process parameters, such as laser power or feed rate, on other target variables has been investigated based on factorial design of experiments (DOE) (Aleksandr et al. 2021; Hofer 2021; Mahamood and Akinlabi 2016; Moradi et al. 2021). Thus, to make efficient use of the technology, it remains to be investigated which process parameters influence the energy demand of the DED-LB process.

In this approach of evaluating the energy consumption of the AM process itself, authors such as (Gao, Wolff, and Wang 2021) have gathered information on the energy consumption of different AM processes (DED-LB, PBF-LB, and BJT among others) while working with different materials (such as metal powder, metal wire, and polymers). They analysed the energy consumption derived from the AM process considering the whole production cycle: mining of raw materials, atomisation of the powder or preparation of the wire, printing, and post-processing. For instance, in the atomisation process, authors concluded that the consumption depends on the material used, presenting a higher consumption for nickel-based alloys.

The total energy consumption in metal AM processes includes the primary input energy, such as the laser source or electric arc to melt the metal materials, alongside the secondary energy used for the machine and system operation (Gisario et al. 2019). During the PBF-LB processes the main energy consumption is based on the system losses and on the secondary energy required for the correct performance of the AM machine. Since these processes involve equipment as preheaters for the printing chamber, coolers, booms, engines, drivers, and screening machines which contribute primarily to the energy consumption. For example, the energy consumption for the whole PBF-LB system is typically 5 to 10 times larger than that of the primary printing process (Liu et al. 2018). Conversely, in DED-LB the consumption associated with the secondary energy is considerably reduced, and the primary deposition energy becomes the principal energy consumption source of the process. In addition, a lower energy consumption for each kg of deposited material is achieved as a result of a higher deposition rate, Figure 1.

Concerning the PBF-LB technology, numerous studies relate the laser energy density to the resulting porosity and mechanical properties (Maamoun et al. 2019; Ma, Wang, and Zeng 2015; Mishurova et al. 2017). Nevertheless, there are no analogous studies for the DED-LB process, in which the influence of process parameters on the energy consumption during deposition is analysed.

In view of this need, the present research work has studied the energy and mass consumption efficiencies of the laser Directed Energy Deposition (DED-LB) process. Firstly, the energy consumption of the laser generator has been experimentally measured for the different operating regimes. Afterwards, in a second step, a design of experiments (DOE) is developed to relate the energy and mass efficiency of the process with the input parameters (laser power, feed rate and mass flow rate). In the present research the scope is focused on the energy and mass efficiency evaluation of the DED-LB process. Therefore, post-processing operations, i.e. machining, are left aside as they are considered mandatory and inevitable regardless of the process parameters used in the deposition process.

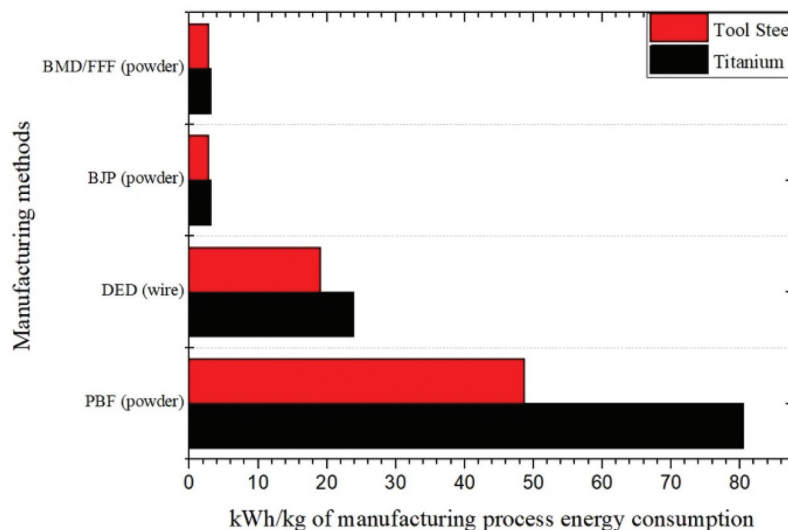


Figure 1. Energy consumption of the different AM processes measured in kWh/kg (Gao, Wolff, and Wang 2021).

## 2. Methodology

The aim of the present work is to quantify the consumption of the laser generator to estimate the energy consumed in the process, since it is the main source of consumption in DED-LB, and hence to achieve a more environmentally responsible manufacturing. The Aktinos 500 laser centre, Figure 2(a), coupled with the Rofin FL010 fibre laser, Figure 2(b), is employed in the experimental tests. The laser has a 1 kW maximum output power and can be operated in both continuous (CW) and pulsed (PWM) modes. When operating the laser in pulsed mode, the pulse shape is controlled by the duty-cycle (DC) and pulse frequency variables, Figure 2(c).

The laser beam has a 1.75 mm diameter at the focal plane, which is situated at a 15 mm distance from the nozzle tip, and the employed nozzle is an in-house manufactured coaxial continuous nozzle. Argon 2X is employed as shielding and carrier gas in all the tests, which is fed with 15 l/min and 5 l/min flow rates, respectively. These parameters are maintained constant in the experimental tests, in order to eliminate their effect on the obtained results. Besides, if test conditions vary, such as substrate surface roughness, substrate temperature, laser incidence angle, or focal distance, the obtained results would not be comparable. Consequently, the same procedure and setup is employed in all tests.

In order to obtain comparable results, in the present work a constant 20 °C room temperature is ensured during the tests

and the substrate is cooled down between individual tests to avoid its overheating and maintain its temperature below 30 °C. Prior to the tests, the AISI 1045 substrate was ground and cleaned with acetone to eliminate any oil and dirt from its surface. The laser is positioned perpendicular to the substrate in all tests.

### 2.1. Experimental tests

The study is carried out in two phases: first, the relationship between the power generated by the laser and the active power consumed from the network is obtained. During these tests, the laser is held static on an aluminium block which works as a heat sink, and the energy consumption is measured for the different test conditions indicated in Table 1

In a second stage and once the laser performance has been characterised, the energy and mass efficiency of the DED-LB deposition process are analysed. For this stage, the tests detailed in Table 2 are carried out, and the cross sections of the single clads are evaluated. Likewise, the laser has been used in continuous mode. Each sample was cut using a metallographic saw and after being individually embedded, they were sanded and polished following a standard metallographic procedure for the material. Moreover, the microstructure of the deposited material was revealed by electrolytic etching with a 10% oxalic acid

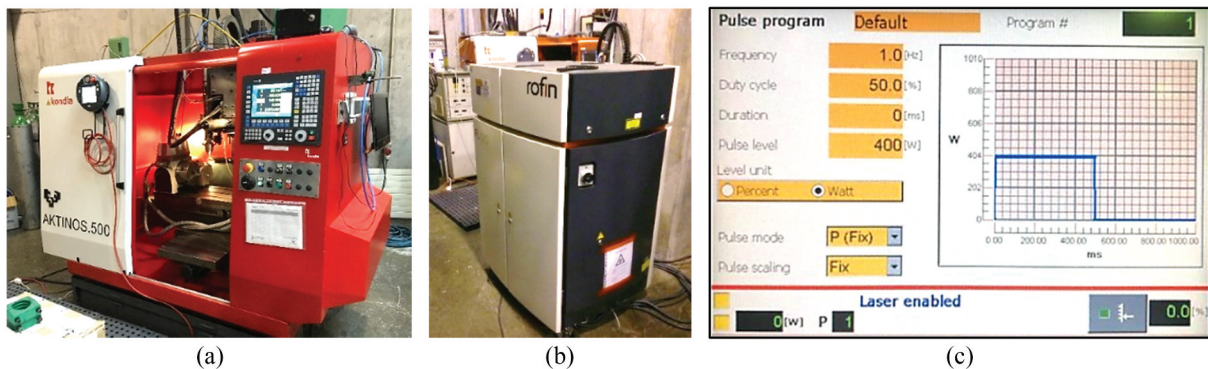


Figure 2. (a) Kondia aktinos 500 laser centre, (b) rofin FL010 laser generator and (c) control screen of the laser with a programmed 50% duty-cycle.

Table 1. Tests performed for the quantification of the energy consumption of the laser generator, where  $P_{nominal}$  is the nominal laser power, and  $f$  and  $t$  are the pulse frequency and duration, respectively.

Test N.	$P_{nominal}$ [W]	DC [%]	$f$ [Hz]	$t$ [s]
1	100	100	0	60
2	200			
3	300			
4	400			
5	500			
6	600			
7	700			
8	800			
9	900			
10	1000			
11	400	50	1	
12	400		100	
13	400		1000	
14	800		1	
15	800		100	
16	800		1000	

**Table 2.** Tests for the quantification of the energy consumption of the laser in the second stage, where  $P$  is the nominal laser power,  $F$  the feed rate and  $M$  the mass rate.

Tests N.	$P_{\text{nominal}}$ [W]	$F$ [mm/min]	$M$ [g/min]
1	800	500	2.98
2	700	400	4.00
3	700	600	4.00
4	900	400	4.00
5	900	600	4.00
6	631	500	5.50
7	800	331	5.50
8	800	500	5.50
9	800	500	5.50
10	800	500	5.50
11	800	500	5.50
12	800	668	5.50
13	968	500	5.50
14	700	400	7.00
15	700	600	7.00
16	900	400	7.00
17	900	600	7.00
18	800	500	8.02

solution and 20 V voltage. Lastly, a Leica DCM3D confocal microscope was used to inspect the sections and to obtain the necessary images for measuring the height, width, depth, and area of the deposited clad.

## 2.2. Employed materials

The substrate employed is a  $70 \times 200 \times 10$  mm<sup>3</sup> AISI 1045 steel billet, whereas the filler material is a cobalt-based alloy, Stellite 6. This alloy is widely employed in the additive manufacturing industry for repairing turbine blades, due to the surface hardness, wear resistance and corrosion protection it offers (Bakhshayesh et al. 2024). Concerning the promising properties of the Stellite 6, it is employed in this study because energy and mass consumption is also of critical importance in the repair industry.

The Stellite 6 filler powder has been manufactured by gas atomisation with a particle size between 45 and 106  $\mu\text{m}$ , which ensures the sphericity of the particles. The chemical

compositions of both materials are listed in Table 3. Also, 2X argon is used both as a shielding gas and as a carrier gas in all tests.

## 2.3. Consumption measurements

The Fluke model 1732 three-phase network analyser has been used to measure the electrical consumptions. This equipment has voltage and current probes, which allow measurements to be taken in all three phases, see Figure 3(a). According to the data sheet of the analyser, the measuring error of the power consumption is below 1%. Moreover, to obtain a consistent value of the active power consumption, several measurements have been done when increasing the laser power and when lowering it. To operate safely, an electrical bridge has been designed, Figure 3(b), which allows the black voltage probes to be connected by means of clamps and the red current probes to be clamped to the different phases with the rings designed for this purpose. In this way, the instantaneous active, reactive, and apparent power can be obtained, Figure 3(c).

Finally, it is worth mentioning that the software Design Expert has been implemented for the generation of the DOE and the analysis of the results. The individual tests carried out are detailed in section 3. Accordingly, the process input variables (laser power, feed rate and powder mass flow rate) have been related to the output variables, being in this case the power consumed by the network, geometrical dimensions and area of the clad supplied, mass efficiency, energy efficiency and dilution.

## 3. Results

### 3.1. Stage 1: analysis of the rofin FL010 laser generator consumption

As indicated in the methodology section, first of all the stable range of the laser in the continuous working mode is analysed. Two averaging sequences were performed and in each one, energy consumption was measured in ascending order (tests

**Table 3.** Chemical composition in weight % of the employed materials (Ostolaza et al. 2020.).

Material	Co	Cr	W	Si	Fe	C	Mo	Mn	P	S	Cu	Ni
Stellite 6	Bal.	28.00	4.00	1.50	3.00	1.00	1.00	0.00	0.00	0.00	0.00	3.00
AISI 1045	0.0	$\leq 0.04$	0.00	$\leq 0.40$	Bal.	0.45	0.00	0.65	$\leq 0.05$	$\leq 0.05$	$\leq 0.04$	$\leq 0.10$

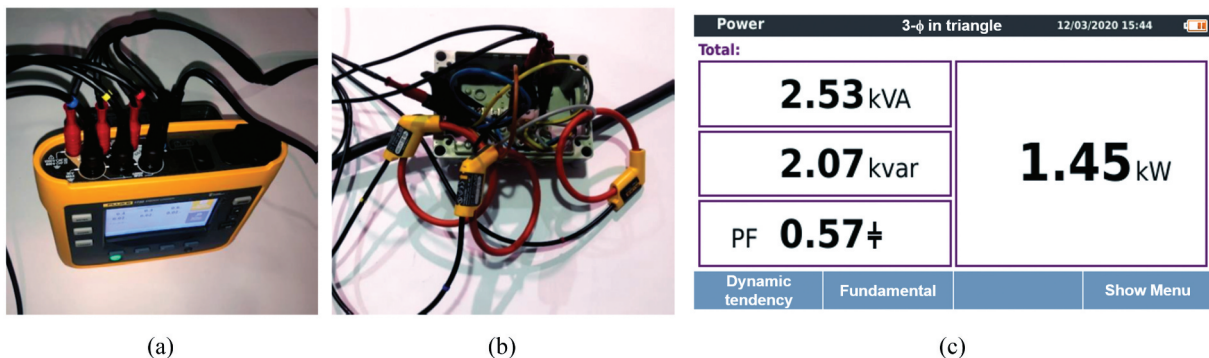


**Figure 3.** (a) Fluke 1732 three-phase analyser, (b) the electrical bridge for connecting it in series with the power supply of the rofin FL010 laser and (c) an example of a reading.

1–10) and descending order (tests 10–1). Therefore, four measurements, 60 second duration each, were carried out for every laser nominal power. The measured values were averaged with a network analyser to obtain the average values.

As it is shown in Figure 4, the laser presents a high residual power consumption and as the output power of the laser increases, the active power consumption of the network increases almost linearly. Best fit is achieved with a second order polynomial trend line, with a  $R^2$  of 0.9997, which equation is included in the same figure.

When the laser generator is connected to the electrical network and mains are enabled, a 0.22 kW active power consumption is detected, but when the laser is enabled, this value increases to 1.45 kW. Prior to the tests, the laser was calibrated using a Coherent PM3K–100 power metre and a power loss of between 8–10% is detected for the whole range. In the present research the laser power will always refer to the nominal power, as well as the variables calculated based on the laser power.

On the assumption that CW operation (equivalent to 100% DC) and operation at twice the power but pulsing at 50% DC, introduce the same amount of energy into the part irradiated by the laser, the active powers consumed in the network have been measured for the situations shown in Table 1. Table 4 summarises the power consumption readings obtained and the energy savings that would be achieved in each case.

As can be seen, when operating in pulsed mode, the active power consumed from the network is reduced between 4% and 9%, the reduction being greater as the pulsing frequency

increases. This active energy saving is based on the results detailed in Figure 4, where higher nominal laser powers provide higher energy efficiencies. Consequently, the use of higher powers in pulsed mode also results in energy savings. In the case of using twice the power than in continuous mode and a pulsed frequency of 1000 Hz, the energy saving achieved is 9% for the same energy input. Figure 5 graphically shows the evolution of the active power consumed from the network as a function of the pulsing frequency. Therefore, it can be concluded that the use of pulsing strategies is a good alternative for reducing the consumption of the DED-LB process.

### 3.2. Stage 2: analysis of the energy and mass efficiency of the DED-LB process

The first task for this second stage was the metallographic analysis of the deposited clads. From each 50 mm long clad, three sections were analysed, the first one situated at 10 mm from the initial point, the second in the centre of the clad, and the third at a 10 mm distance from the end point. In Figure 6 an example of each clad is shown. Most of them present a good appearance, free of internal defects, and none of them show cracking or lack of adhesion with the substrate.

In some tests, such as 12 and 13 in the provided cross sections in Figure 6, surface cavities are found because non-melted particles have been torn off during the metallographic procedure. This is generated because lower laser powers can generate the adhesion of non-melted powder particles to the upper part of the clad. Nevertheless, if a new layer

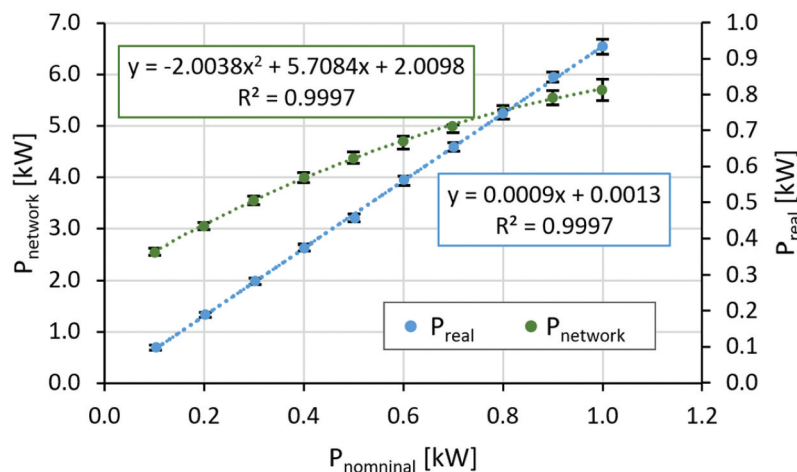


Figure 4. Relationship between the nominal power of the laser,  $P_{\text{nominal}}$ , the active power consumed by the laser generator for CW operation,  $P_{\text{network}}$ , and the measured real laser power,  $P_{\text{real}}$ .

Table 4. Relationship between laser power and active power consumed from the grid,  $P_{\text{network}}$ , for different powers and duty cycles.

$P_{\text{nominal}}$ [W]	DC [%]	f [Hz]	$P_{\text{network}}$ [kW]	Energy savings [%]
200	100	0	3.09	0.00
400	50	1	2.96	4.05
400	50	100	2.94	4.57
400	50	1000	2.80	9.30
400	100	0	3.99	0.00
800	50	1	3.69	7.60
800	50	100	3.73	6.47
800	50	1000	3.73	9.06

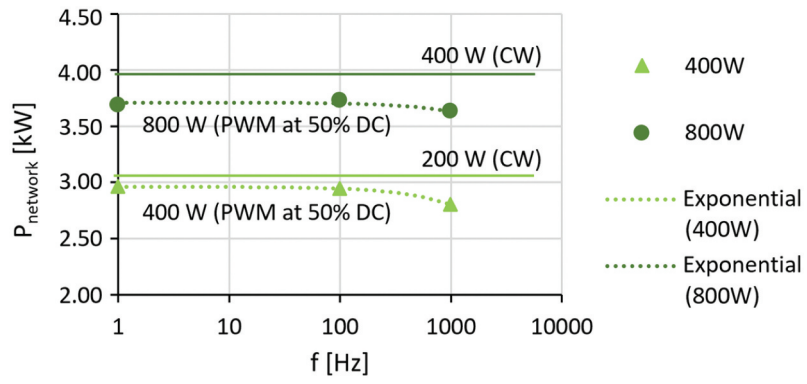


Figure 5. Relationship between the pulsing frequency and the active power consumed from the network,  $P_{network}$ , for different laser powers and frequencies operating in PWM.

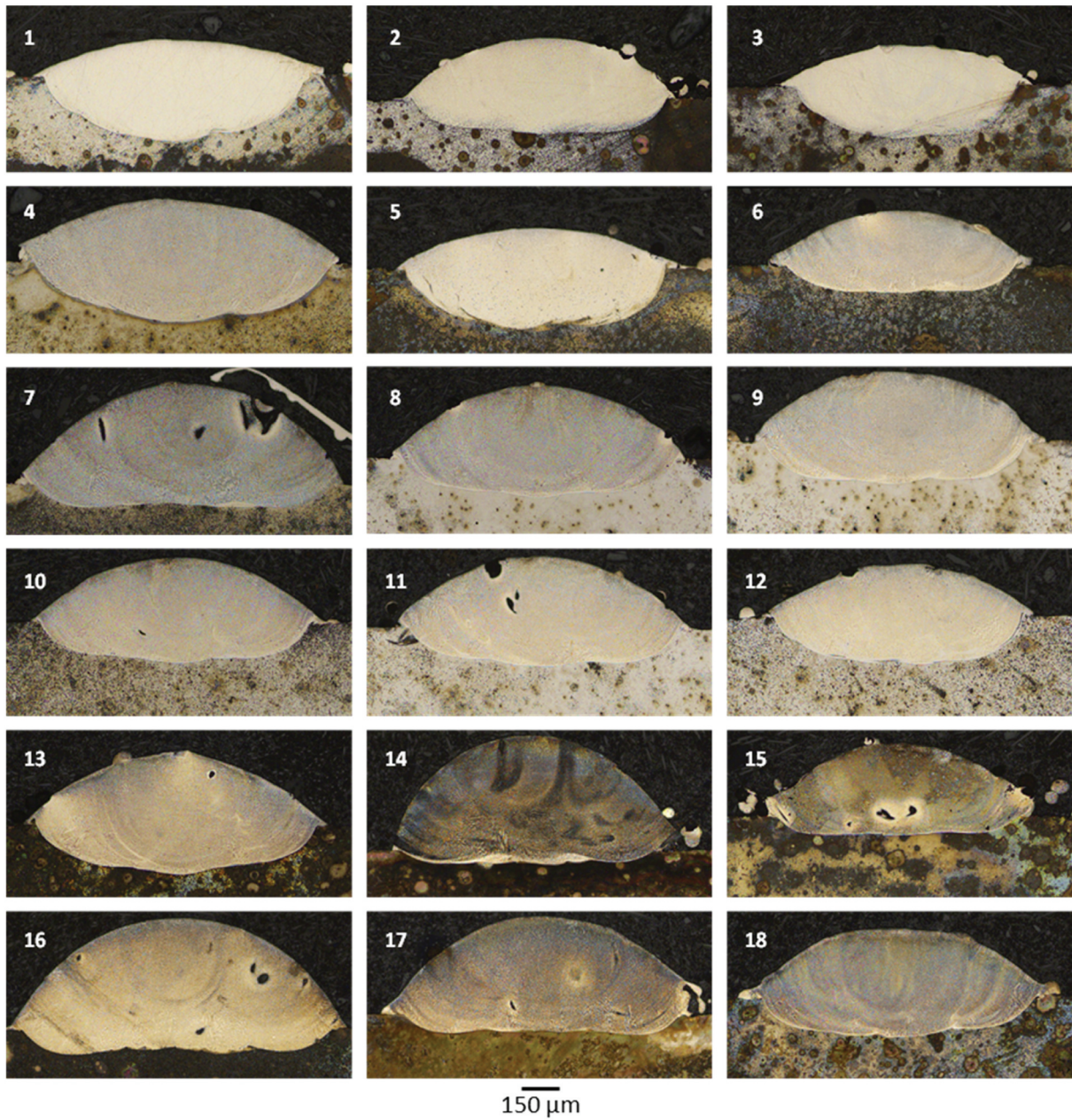


Figure 6. Cross sections of the deposited stellite 6 clads.

is deposited on top of the previous, these particles are melted and therefore, the problem is avoided. In case no upper layers are deposited, that means that this surface needs to be machined to ensure part accuracy and surface roughness, what also eliminates the problem.

On the contrary, those tests in which the filler material mass rate is maximised, a higher amount of internal porosity is detected. In all cases, the measured porosity does not exceed the 3% of the whole cross section area. However, in test 15 lack of fusion defects have been found in all the three analysed cross sections, which means that there is not enough laser power, 700W, in combination with the employed feed rate and mass rate, 600 mm/min and 7.0 g/min, respectively, to melt correctly all the filler material. Consequently, if high mass rates are desired, laser power needs to be increased accordingly.

Worst clad quality is obtained in Test 7, which corresponds to the lower feed rate, 331 mm/min. Therefore, the internal voids and porosity detected in the three analysed cross sections are attributed to it. These defects would affect the mechanical performance of the component, especially at tensile stress situations, where cracks may initiate on them. Therefore, the parameter window corresponding to Test 7 is considered unacceptable.

The results of the metallographic analysis and the quantification of energy and mass efficiency are shown in Table 5. To facilitate the understanding, the output variables shown in the table are defined below:

Height, width, depth, and areas of the deposited clad, defined as H, W, D, and A1 and A2 in Figure 7, respectively. Their values are calculated as mean values of the analysed three cross sections.

- Mass efficiency ( $\eta_m$ ): indicates the percentage of powder that becomes part of the clad, relative to the amount of material fed into the process. A1 is the upper area of the clad,  $\rho$  is the Stellite 6 density, M the mass rate, and F the feed rate. Its value is calculated as a mean value of the analysed three cross sections.

$$\eta_m = \frac{A1 \cdot \rho}{M/F} \cdot 100 \quad (1)$$

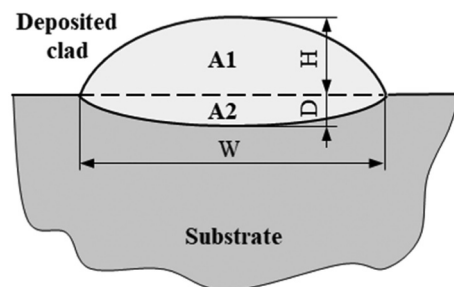
- Energy efficiency of the process ( $\eta_e$ ): shows the amount of energy that needs to be used in the process for each gram of material that becomes part of the final clad. Its value is calculated as a mean value of the analysed three cross sections.

$$\eta_e = \frac{P/F}{A1 \cdot \rho} \quad (2)$$

- Dilution: defines the ratio between the lower clad area, A2, and the upper clad area, A1, based on the equation shown in Figure 7. Its value is calculated as a mean value of the analysed three cross sections.

Table 5. Summary of the clad dimensions, energy consumption, and efficiency of the DED-LB process.

Test	$P_{nominal}$ [W]	F [mm/min]	M [g/min]	$P_{network}$ [kW]	W [mm]	H [mm]	D [mm]	H/W [-]	A1 [mm <sup>2</sup> ]	A2 [mm <sup>2</sup> ]	$\eta_m$ [%]	$\eta_e$ [kWh/kg]	Dil. [%]
1	800	500	2.98	5.09	1.48	0.18	0.34	0.12	0.18	0.35	26.08	109.25	65.67
2	700	400	4.00	4.91	1.44	0.30	0.19	0.20	0.30	0.20	25.57	80.00	40.12
3	700	600	4.00	4.7	1.27	0.22	0.25	0.17	0.20	0.21	25.19	77.73	51.46
4	900	400	4.00	5.41	1.60	0.29	0.31	0.18	0.33	0.35	27.43	82.18	51.49
5	900	600	4.00	5.42	1.48	0.20	0.33	0.14	0.23	0.34	28.99	77.90	59.68
6	631	500	5.50	4.69	1.27	0.27	0.13	0.22	0.26	0.13	20.18	70.43	32.56
7	800	331	5.50	5.13	1.66	0.50	0.13	0.30	0.58	0.14	29.36	52.95	19.61
8	800	500	5.50	5.19	1.54	0.33	0.20	0.21	0.35	0.21	26.85	58.56	37.39
9	800	500	5.50	5.18	1.49	0.29	0.25	0.19	0.30	0.25	22.94	68.42	45.54
10	800	500	5.50	5.12	1.47	0.34	0.22	0.23	0.34	0.23	25.78	60.18	40.64
11	800	500	5.50	5.12	1.55	0.36	0.16	0.23	0.37	0.20	28.31	54.80	34.81
12	800	668	5.50	5.03	1.38	0.24	0.27	0.18	0.25	0.26	26.04	58.54	50.78
13	968	500	5.50	5.65	1.58	0.31	0.26	0.20	0.33	0.29	25.32	67.62	46.77
14	700	400	7.00	4.81	1.39	0.56	0.08	0.40	0.61	0.09	29.47	38.86	12.34
15	700	600	7.00	4.67	1.34	0.36	0.11	0.27	0.32	0.11	23.22	47.88	25.35
16	900	400	7.00	5.46	1.76	0.56	0.13	0.32	0.68	0.17	32.75	39.70	19.55
17	900	600	7.00	5.42	1.61	0.49	0.11	0.30	0.57	0.11	40.87	31.57	16.42
18	800	500	8.02	5.15	1.52	0.37	0.18	0.24	0.40	0.19	21.15	50.60	32.32



$$Dilution = \frac{A2}{(A1 + A2)} \cdot 100$$

Figure 7. Definition of the dilution and characterization of the clad dimensions.

$$Dil = \frac{A2}{(A1 + A2)} \cdot 100 \quad (3)$$

### 3.3. DOE results

The analysis of the results has been performed employing a Response Surface Methodology (RSM). This method is based on the construction of polymeric equations (first or second order) relating the input and output variables. The RSM is commonly employed in additive manufacturing studies with the aim of obtaining an effective relationship among different parameters (Alizadeh-Sh et al. 2020).

Based on the value of the post-analysis coefficient 'p' and the value of the correlation 'R2' obtained in the analysis of the results, it has been concluded that for the case of mass efficiency it is convenient to use a quadratic approximation, while for the energy consumption efficiency a better approximation is obtained by using a linear relationship between the parameters.

Figure 8 shows the evolution of mass efficiency in relation to the feed rate and the laser power. Thus, it can be concluded that higher laser powers lead to a better powder entrapment efficiency. For example, for a mass flow rate of 7 g/min and a constant feed rate of 600 mm/min, varying the power from 700 to 900 W increases the mass efficiency by 50%. In addition, the increase of the feed rate also results in an increase of the mass efficiency. Higher efficiency improvements are obtained at high mass rates, but it must be kept in mind that if the laser power is not capable of melting the material being fed, internal defects will appear.

In the case of the feed rate, there is no direct relationship between this variable and the mass efficiency. At low laser powers, an increase in the feed rate decreases the percentage of powder trapped in the melt pool, while, at high powers, the tendency is opposite.

Regarding the energy efficiency, Figure 9, an increase in the powder mass rate drastically reduces the energy consumption per gram of material that becomes part of the clad. In contrast,

it is concluded that laser power and feed rate have little influence on this parameter.

Similarly, the dilution value has been plotted with respect to the feed rate and power used for the cases of 4 and 7 g/min powder delivery mass rates, Figures 10 (a,b), respectively. As can be seen, the dilution increases slightly with the laser power, as the amount of material melted by the laser increases. For the case of the feed rate, the increase of the dilution with respect to the speed is mainly due to the decrease of the upper area of the deposited clad (A1). Finally, it should be noted that the parameter that has the greatest influence on dilution is the mass rate, where an increase in the rate results in a reduction of dilution.

Consequently, if both parameters, mass efficiency and energy consumption, are to be optimised, it is advisable to use high power and powder flow rates. However, it must be taken into account that these parameters can affect the dilution of the generated clad, which is a limiting factor when modifying the input parameters of the DED-LB process.

### Conclusions

In the present research work, the energy efficiency of an industrial laser has been studied, and its behaviour has been subsequently analysed in the context of the DED-LB deposition process. The most relevant conclusions reached after analysing the results are the following:

- The Rofin FL010 laser has a high residual power consumption due to the pumping of the active medium. However, when working with the laser in continuous mode (CW) the variation of the active power consumed from the network is practically linear concerning the emitted laser power. Therefore, the use of higher laser powers results in better energy efficiency of the laser generator.
- It has been concluded that the use of the laser in pulsed mode (PWM) is a good alternative to reduce the energy consumption of the DED-LB process. The influence of

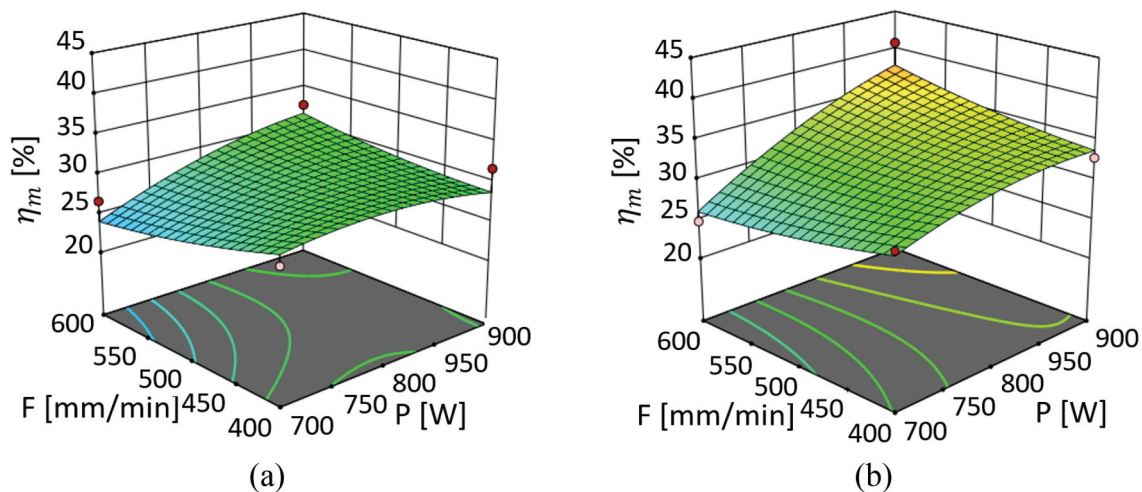


Figure 8. Efficiency of the energy consumption of the process for mass rates of 4 g/min (a) and 7 g/min (b).

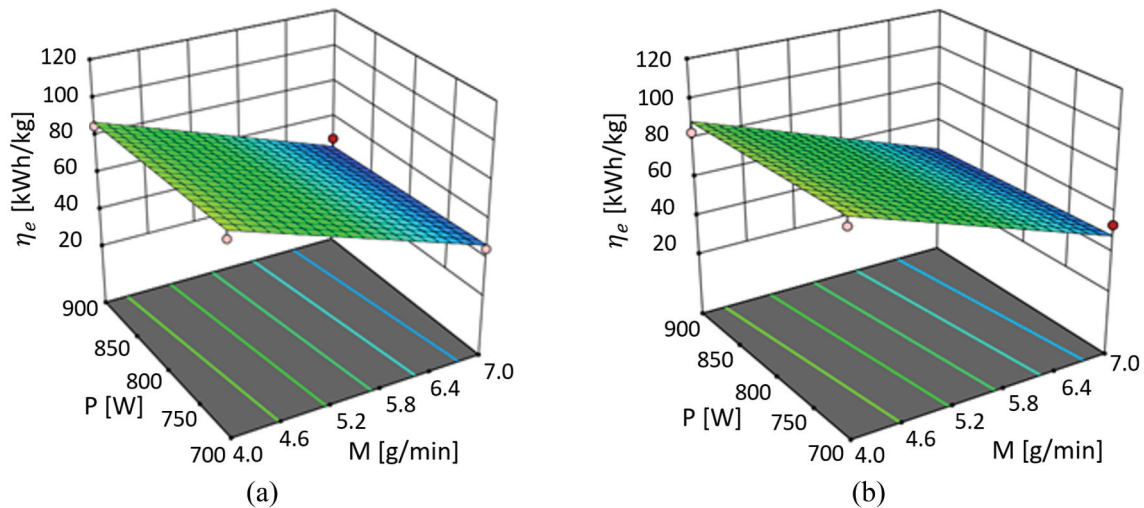


Figure 9. Efficiency of the energy consumption of the process for feed rates of 400 m/min (a) and 600 m/min (b).

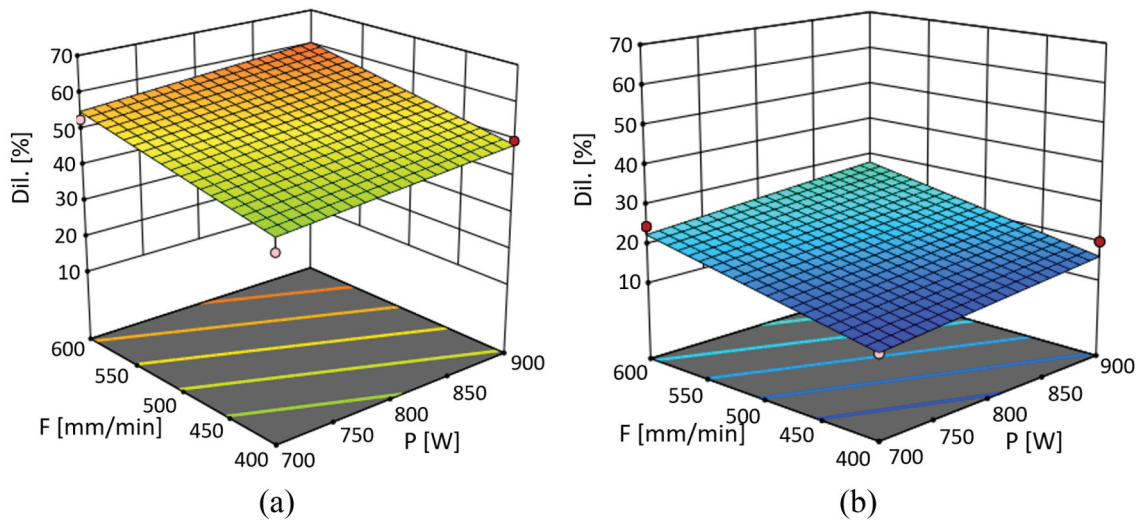


Figure 10. Dilution of the deposited material for mass flow rates of 4 g/min (a) and 7 g/min (b).

the pulsed mode on the quality and properties of the deposited material needs to be studied further, but given that reductions in consumption of up to 9% have been obtained, this manufacturing alternative opens the door to a more energy-efficient process.

Finally, once the results from the DOE have been analysed and the relationship between input and output parameters has been established, the following conclusions have been drawn for the DED-LB process when the laser is employed in the continuous mode:

- The mass efficiency depends mainly on the laser power used. It has been observed that a power increase generates a larger melt pool, which facilitates the powder entrapment and increases the mass efficiency of the process.
- In the case of the energy efficiency, the most influential variable is the powder mass rate. A higher mass rate results in a more efficient use of the laser power, thus

reducing the amount of energy required per gram of material that becomes part of the deposited clad.

- It has been found that the dilution depends mainly on the mass flow, where an increase in the amount of material deposited per time unit results in a larger upper area of the deposited clad (A1) and, therefore, a lower dilution.

After the present research, the characterisation of the properties of the materials additively manufactured under optimal conditions of mass and energy efficiency is established as future work. Since it should be ensured that the most efficient parameters do not negatively affect the performance of the resulting component.

### Acknowledgments

Grant TED2021-130543B-I00 funded by the MCIN/AEI/10.13039/501100011033 and the European Union NextGenerationEU/PRTR, and Grant PID2022-141946OB-C21 funded by MCIN/AEI/10.13039/501100011033/and by ERDF A way of making Europe.

## Disclosure statement

No potential conflict of interest was reported by the author(s).

## Funding

This work was supported by the Ministerio de Ciencia e Innovación [ALASURF (PID2019-109220RB-I00)].

## Notes on contributors

**J.I. Arrizubieta** is an Associate Professor at the University of the Basque Country and lectures at the Engineering School of Bilbao. He finished his PhD thesis in 2017 in laser additive manufacturing and since then has been researching in the field. He is an active member of the Aeronautics Advanced Manufacturing Center (CFAA), and has participated in several international and national projects, as well as published more than 30 international peer reviewed journals.

**O. Murua** started her career in 2014 at the Bilbao School of Engineering (UPV/EHU), where finally obtained the Master Degree in Industrial Engineering. Currently, she is realizing her PhD Studies about the modelling of laser processes within the High-Performance Manufacturing Group. Moreover, after being involved in different international projects; such as ADDITOOL, and conferences (LANE 2022 and MESIC 2023), she has also accomplished an International 3 months stay in the AMEC centre of Siemens.

**A. Urresti** is a PhD student at the Mechanical Department of the University of the Basque Country. She finished her MSc in 2022 and since then she has been researching in the Additive Manufacturing field. She is a Member of the High Performance Manufacturing Group and her research interests are focused mainly in multimaterial and multistructural Laser Directed Energy Deposition.

**O. Ukar** is an Associate Professor at University of Deusto and Vice-Dean for Student Affairs, and she lectures at the Engineering Faculty. She finished her PhD thesis in 2007 in Electrical Grounding Systems and since then her research work have been related to energy efficiency, renewable energies and electricity market.

## ORCID

J.I. Arrizubieta  <http://orcid.org/0000-0002-6030-4941>

O. Murua  <http://orcid.org/0000-0002-2058-3042>

A. Urresti  <http://orcid.org/0000-0002-1768-8206>

O. Ukar  <http://orcid.org/0000-0002-9387-1096>

## Author contributions

J.I.A.: conceptualisation; methodology; validation; visualisation; writing – original draft; writing – review and editing. O.M.: validation; writing – reviewing and editing. A.U.: validation; writing – reviewing and editing. O.U.: methodology; data curation; writing – reviewing and editing

## Data availability statement

The authors confirm that the data supporting the findings of this study are available within the article.

## References

Aleksandr, K., S. Ferdinando, R. Joel, C. Joel, M. Jordan, and J. Thomas. 2021. “Effect of Direct Energy Deposition Parameters on Morphology, Residual Stresses, Density, and Microstructure of 1.2709 Maraging Steel.” *The International Journal of Advanced Manufacturing Technology* 117 (3): 1287–1301. <https://doi.org/10.1007/s00170-021-07635-w>.

- Alizadeh-Sh, M., S. P. H. Marashi, E. Ranjbarnodeh, R. Shoja-Razavi, and J. P. Oliveira. 2020. “Prediction of Solidification Cracking by an Empirical-Statistical Analysis for Laser Cladding of Inconel 718 Powder on a Non-Weldable Substrate.” *Optics & Laser Technology* 128:106244. <https://doi.org/10.1016/j.optlastec.2020.106244>.
- Arrizubieta, J. I., O. Ukar, M. Ostolaza, and A. Mugica. 2020. “Study of the Environmental Implications of Using Metal Powder in Additive Manufacturing and Its Handling.” *Metals* 10 (2): 261. <https://doi.org/10.3390/met10020261>.
- Bakhshayesh, M. M., F. Khodabakhshi, M. H. Farshidianfar, Š. Nagy, M. Mohammadi, and G. Wilde. 2024. “Additive Manufacturing of Stellite 6 Alloy by Laser-Directed Energy Deposition: Engineering the Crystallographic Texture.” *Materials Characterization* 207:113511. <https://doi.org/10.1016/j.matchar.2023.113511>.
- Ehmsen, S., M. Glatt, and J. C. Aurich. 2023. “Influence of Process Parameters on the Power Consumption of High-Speed Laser Directed Energy Deposition.” *Procedia CIRP* 116:89–94. <https://doi.org/10.1016/j.procir.2023.02.016>.
- Felice, I. O., J. Shen, A. F. C. Barragan, I. A. B. Moura, B. Li, B. Wang, H. Khodaverdi, et al. 2023. “Wire and Arc Additive Manufacturing of Fe-Based Shape Memory Alloys: Microstructure, Mechanical and Functional Behavior.” *Materials & Design* 231:112004. <https://doi.org/10.1016/j.matdes.2023.112004>.
- Ferreira, I. A., J. P. Oliveira, J. Antonissen, and H. Carvalho. 2023. “Assessing the Impact of Fusion-Based Additive Manufacturing Technologies on Green Supply Chain Management Performance.” *Journal of Manufacturing Technology Management* 34 (1): 187–211. <https://doi.org/10.1108/JMTM-06-2022-0235>.
- Gao, C., S. Wolff, and S. Wang. 2021. “Eco-Friendly Additive Manufacturing of Metals: Energy Efficiency and Life Cycle Analysis.” *Journal of Manufacturing Systems* 60:459–472. <https://doi.org/10.1016/J.JMSY.2021.06.011>.
- Gisario, A., M. Kazarian, F. Martina, and M. Mehrpouya. 2019. “Metal Additive Manufacturing in the Commercial Aviation Industry: A Review.” *Journal of Manufacturing Systems* 53:124–149. <https://doi.org/10.1016/J.JMSY.2019.08.005>.
- Hoefer, K. 2021. “Correlations Between Process and Geometric Parameters in Additive Manufacturing of Austenitic Stainless Steel Components Using 3DPMD.” *Applied Sciences* 11 (12). <https://doi.org/10.3390/app11125610>.
- Huang, R., M. Riddle, D. Graziano, J. Warren, S. Das, S. Nimbalkar, J. Cresko, and E. Masanet. 2016. “Energy and Emissions Saving Potential of Additive Manufacturing: The Case of Lightweight Aircraft Components.” *Journal of Cleaner Production* 135:1559–1570. <https://doi.org/10.1016/j.jclepro.2015.04.109>.
- ISO/ASTM. 2021. *ISO/ASTM 52900. Additive Manufacturing—General Principles—Fundamentals and Vocabulary*.
- Jackson, M. A., A. Van Asten, J. D. Morrow, S. Min, and F. E. Pfefferkorn. 2016. “A Comparison of Energy Consumption in Wire-Based and Powder-Based Additive-Subtractive Manufacturing.” *Procedia Manufacturing* 5:989–1005. <https://doi.org/10.1016/j.promfg.2016.08.087>.
- Khalid, M., and Q. Peng. 2021. “Investigation of Printing Parameters of Additive Manufacturing Process for Sustainability Using Design of Experiments.” *Journal of Mechanical Design* 143 (3). <https://doi.org/10.1115/1.4049521>.
- Liu, Z. Y., C. Li, X. Y. Fang, and Y. B. Guo. 2018. “Energy Consumption in Additive Manufacturing of Metal Parts.” *Procedia Manufacturing* 26:834–845. <https://doi.org/10.1016/J.PROMFG.2018.07.104>.
- Maamoun, A. H., Y. F. Xue, M. A. Elbestawi, and S. C. Veldhuis. 2019. “The Effect of Selective Laser Melting Process Parameters on the Microstructure and Mechanical Properties of Al6061 and AlSi10mg Alloys.” *Materials* 12 (1): 12. <https://doi.org/10.3390/ma12010012>.
- Maddison, A. 2007. *Contours of the World Economy 1-2030 AD: Essays in Macro-Economic History*. New York, United States: Oxford University Press.

- Mahamood, R. M., and E. T. Akinlabi. 2016. "Processing Parameters Optimization for Material Deposition Efficiency in Laser Metal Deposited Titanium Alloy." *Lasers in Manufacturing and Materials Processing* 3 (1): 9–21. <https://doi.org/10.1007/s40516-015-0020-5>.
- Ma, M., Z. Wang, and X. Zeng. 2015. "Effect of Energy Input on Microstructural Evolution of Direct Laser Fabricated IN718 Alloy." *Materials Characterization* 106:420–427. <https://doi.org/10.1016/J.MATCHAR.2015.06.027>.
- Mishurova, T., S. Cabeza, K. Artzt, J. Haubrich, M. Klaus, C. Genzel, G. Requena, and G. Bruno. 2017. "An Assessment of Subsurface Residual Stress Analysis in SLM Ti-6Al-4V." *Materials* 10 (4): 348. <https://doi.org/10.3390/ma10040348>.
- Moradi, M., A. Hasani, Z. Pourmand, and J. Lawrence. 2021. "Direct Laser Metal Deposition Additive Manufacturing of Inconel 718 Superalloy: Statistical Modelling and Optimization by Design of Experiments." *Optics & Laser Technology* 144:107380. <https://doi.org/10.1016/j.optlas tec.2021.107380>.
- Najmon, J. C., S. Raeisi, and A. Tovar. 2019. "Review of Additive Manufacturing Technologies and Applications in the Aerospace Industry." *Additive Manufacturing for the Aerospace Industry* 7–31. <https://doi.org/10.1016/B978-0-12-814062-8.00002-9>.
- Nickels, L. 2015. "AM and Aerospace: An Ideal Combination." *Metal Powder Report* 70 (6): 300–303. <https://doi.org/10.1016/J.MPRP.2015.06.005>.
- Ostolaza, M., J. I. Arrizubieta, M. Cortina, and A. Lamikiz. 2020. "Study of the Reinforcement Phase Dilution into the Metal Matrix in Functionally Graded Stellite 6 and WC Metal Matrix Composite by Laser Metal Deposition." *Procedia CIRP* 94:330–335. <https://doi.org/10.1016/J.PROCIR.2020.09.062>.
- Peng, T., J. Lv, A. Majeed, and X. Liang. 2021. "An Experimental Investigation on Energy-Effective Additive Manufacturing of Aluminum Parts via Process Parameter Selection." *Journal of Cleaner Production* 279:123609. <https://doi.org/10.1016/j.jclepro.2020.123609>.
- Schwerz, C., F. Schulz, E. Natesan, and L. Nyborg. 2022. "Increasing Productivity of Laser Powder Bed Fusion Manufactured Hastelloy X Through Modification of Process Parameters." *Journal of Manufacturing Processes* 78:231–241. <https://doi.org/10.1016/J.JMAPRO.2022.04.013>.
- Tan, C., F. Weng, S. Sui, Y. Chew, and G. Bi. 2021. "Progress and Perspectives in Laser Additive Manufacturing of Key Aeroengine Materials." *International Journal of Machine Tools and Manufacture* 170:103804. <https://doi.org/10.1016/J.IJMACHTOOLS.2021.103804>.
- Wippermann, A., T. G. Gutowski, B. Denkena, M.-A. Dittrich, and Y. Wessarges. 2020. "Electrical Energy and Material Efficiency Analysis of Machining, Additive and Hybrid Manufacturing." *Journal of Cleaner Production* 251:119731. <https://doi.org/10.1016/j.jclepro.2019.119731>.
- Yang, Y., L. Li, Y. Pan, and Z. Sun. 2017. "Energy Consumption Modeling of Stereolithography-Based Additive Manufacturing Toward Environmental Sustainability." *Journal of Industrial Ecology* 21 (S1): S168–S178. <https://doi.org/10.1111/jiec.12589>.